Evaporation from Extensive Surfaces of Water

Evaporation from Extensive Surfaces of Water

By Junsei Kondo

Abstract

Using the theory of turbulent transfer in non-neutral conditions and the empirical relations derived from many observations, a diagram is obtained. By this diagram the evaluations of the evaporation, the turbulent flux of heat and the surface stress can be made from the usual simple observations of wind, air temperature, humidity at a certain level above the water surface, and of the surface temperature.

1 Introduction

Many studies on the energy and mass transfers between the atmosphere and extensive surfaces of water have hitherto been made. However, if one attempts to evaluate the surface stress or the evaporation by the simple observations of wind and humidity usually made by ships, he has no information about the reliable values of the roughness parameter or the stress coefficient and the evaporation coefficient. These values reported from various observations differ in magnitude, (Rossby and Montgomery (1936), Brocks (1955), Hay (1955) and etc.]; this is caused by that the observations of wind or humidity profiles over the water surface are laborious.

Furthermore, if one will calculate the evaporation or the turbulent heat flux in the non-neutral condition by any turbulent theory, [Kao (1959), Yamamoto (1959), Syōno and Hamuro (1962) and etc.], he needs observations of wind, humidity and air temperature at more than three levels; however, these observations are usually difficult.

The author has arranged many observations hitherto made, and taking the atmospheric stability into consideration, he shows a new diagram for the calculation of the evaporation. This may also be used to calculate the surface stress and the turbulent flux of heat.

2 Notations

The following notations are used:

U -wind speed

χ -water vapour concentration

θ -potential temperature

T -absolute temperature

χ_0 -water vapour concentration at height z_0 (extrapolated value)

χ_s -saturated water vapour concentration at the temperature of the surface of the water

θ_0 -potential temperature at height z_0 (extrapolated value)

θ_s -surface temperature of the water
τ -shear stress
E -rate of evaporation
q -turbulent heat flux
u_* -friction velocity
γ^2 -stress coefficient
Γ -evaporation coefficient
k -von Kármán's constant
z_0 -roughness height
ζ_0 -stability parameter
σ -numerical factor
g -acceleration due to gravity
ν -kinematic viscosity of air
C_p -specific heat of air
ρ -air density
The subscripts 1 and 2 represent the heights z_1 and z_2, respectively.

3 Theoretical relations

Equations of the evaporation and the surface stress are given by

$$E = -K\frac{d\chi}{dz}, \tag{1}$$

$$\frac{\tau}{\rho} = {u_*}^2 = K\frac{du}{dz} \tag{2}$$

From Eqs. (1) and (2) we have

$$\left.\begin{aligned} E &= -{u_*}^2\frac{\chi_2-\chi_1}{u_2-u_1} \\ &= {u_*}^2\frac{\chi_0-\chi_1}{u_1} \end{aligned}\right\} \tag{3}$$

or

$$\frac{E}{(1-\varepsilon)(\chi_s-\chi_1)} = \frac{{u_*}^2}{u_1}, \tag{4}$$

where

$$\varepsilon = \frac{\chi_s-\chi_0}{\chi_s-\chi_1} \tag{5}$$

If we assume the neutral condition, then the wind profile is the logarithmic form,

$$\frac{ku}{u_*} = ln\frac{z}{z_0}, \tag{6}$$

therefore Eq. (3) becomes

$$\frac{E}{\chi_1 - \chi_2} = k^2 \frac{u_2 - u_1}{(ln\, z_2/z_1)^2} \tag{7}$$

This is the best known evaporation formula derived by THORNTHWAIT and HOLZMAN (1939). Or, defining for convenience,

$$\Gamma_1 = -\frac{1}{\chi_s - \chi_1} \frac{d\chi}{d\, ln\, z} = -\frac{1}{\chi_s - \chi_1} \frac{\chi_1 - \chi_0}{ln\, z_1/z_0} \tag{8}$$

$$= (1 - \varepsilon) \frac{1}{ln\, z_1/z_0}\,, \tag{9}$$

we have from Eq. (3)

$$\frac{E}{\chi_s - \chi_1} = \frac{k^2 \Gamma_1 u_1}{ln\, z_1/z_0} \tag{10}$$

Evaporation coefficient, Γ_1, was originally used by MONTGOMERY (1940). Next, we will define a new constant $z_{0(\chi)}$, which is expressed in the equation,

$$\chi - \chi_s \propto ln \frac{z}{z_{0(\chi)}} \tag{11}$$

then

$$\Gamma_1 = \left(ln \frac{z_1}{z_{0(\chi)}} \right)^{-1}, \tag{12}$$

and Eq. (10) becomes

$$\frac{E}{\chi_s - \chi_1} = \frac{k^2 u_1}{ln \frac{z_1}{z_0} \cdot ln \frac{z_1}{z_{0(\chi)}}} \tag{13}$$

Above Eqs. (6)–(13) hold only in neutral conditions.

From YAMAMOTO's theoretical equations in non-neutral conditions (1959),

$$\left.\begin{aligned} \frac{k u_1}{u_*} &= -\frac{k(\theta_1 - \theta_0)}{\theta_*} \equiv f_{\xi_1}(\zeta_0) \\ \frac{z_0}{\zeta_0} &= \frac{T u_*^2}{\sigma k g \theta_*}\,, \qquad \theta_* = \frac{q/c_p \rho}{u_*} \end{aligned}\right\} \tag{14}$$

we have

$$\sigma z_0 (1 - \varepsilon') \frac{g}{T} \frac{\theta_1 - \theta_s}{u_1^2} = -\frac{\zeta_0}{f_{\xi_1}(\zeta_0)}\,, \tag{15}$$

where

$$\varepsilon' = \frac{\theta_S - \theta_0}{\theta_S - \theta_1}\,, \qquad \xi_1 = \frac{z_1}{z_0} \tag{16}$$

and σ is a factor to be determined from the observations, in this paper $\sigma=13$ is used [KONDO (1962)].

Then the stability parameter, ζ_0, may be obtained from the observations of u_1, θ_1 and θ_s. And inserting (14) into (4) we have

$$\frac{E}{(1-\varepsilon)(\chi_s-\chi_1)}=\frac{k^2 u_1}{f^2_{\xi_1}(\zeta_0)} \tag{17}$$

The theoretical values of f are given in YAMAMOTO's paper (1959). Recently, KONDO (1962) showed that YAMAMOTO's theoretical profile does not agree with the observation in the very stable condition, so in this case ($\zeta<-2$) we will use the empirical formula of f. Theoretical and empirical values of f are listed in Table 1. From Eqs. (15), (17) and the empirical values of z_0, ε and ε' we can make a diagram for the calculation of the evaporation.

Table 1. Values of f (see 51 p. of KONDO's paper)

$\zeta_0>0$ (unstable)		$\zeta_0<0$ (stable)		
$\zeta=\zeta_0\frac{z}{z_0}$	$f-ln\frac{0.01}{\zeta_0}$	$\zeta=\zeta_0\frac{z}{z_0}$	$f-ln\frac{-0.01}{\zeta_0}$	
	(theory)		(theory)	(observation)
0.01	0	−0.01	0	
0.03	1.09	−0.03	1.10	
0.1	2.28	−0.1	2.33	
0.3	3.33	−0.3	3.48	
1	4.40	−1	4.92	4.92
3	5.17	−3	(7.10)	7.03
6	5.58	−6	(10.12)	9.10
10	5.88	−10	(14.12)	11.05
30	6.29	−30	(34.12)	16.35
60	6.49	−60	(64.12)	20.45
100	6.61	−100	(104.12)	23.6
300	6.80	−300	(304.12)	30.5

4 Empirical relations

Figs. 1 and 2 show the relationships between u/u_1 and $(\chi-\chi_s)/(\chi_1-\chi_s)$, and u/u_1 and $(\theta-\theta_s)/(\theta_1-\theta_s)$ respectively.

In this study, the data were arranged into several groups according to the range of stability conditions, then the mean values of each group were plotted.

Zeros of ordinate, $(u/u_1=0)$, in Figs. 1 and 2 are the extrapolated values at the height z_0, so that the value of each abscissa at this point is ε or ε' respectively. From these figures we may assume,

$$\left.\begin{aligned} &\varepsilon \fallingdotseq 0\ , \quad \varepsilon' \fallingdotseq 0\ , \\ \text{that is}\quad &ln\, z_0 \fallingdotseq ln\, z_{0(\chi)}\ , \quad ln\, z_0 \fallingdotseq ln\, z_{0(\theta)}\ , \\ \text{or}\quad &\chi_0 \fallingdotseq \chi_s\ , \quad \theta_0 \fallingdotseq \theta_s\ , \end{aligned}\right\} \tag{18}$$

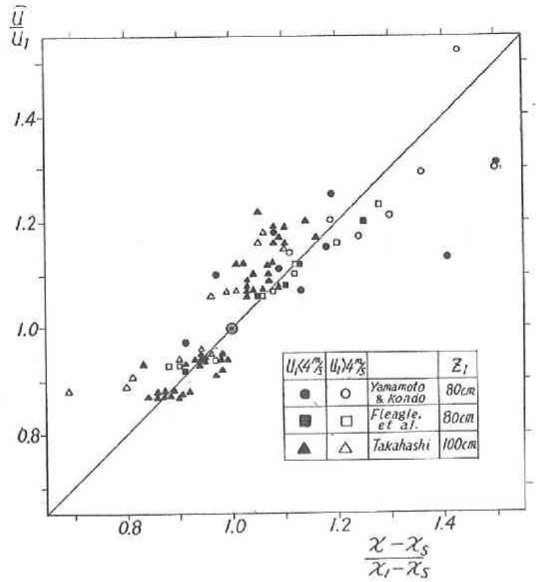

Fig. 1. Relationship between wind-speed and water-vapour pressure profiles.

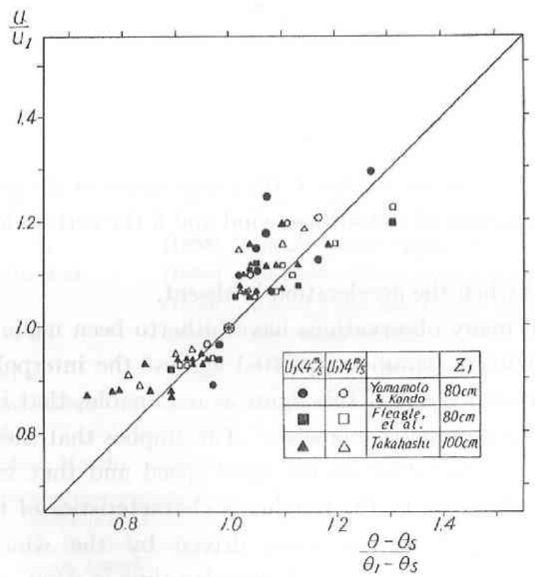

Fig. 2. Relationship between wind-speed and temperature profiles.

where $z_{0(\theta)}$ is defined in the neutral condition as $\theta-\theta_s \propto ln\,(z/z_{0(\theta)})$. These relations (18) will be used later.

In neutral conditions, the roughness height, z_0, the stress coefficient, γ^2, and the evaporation coefficient, Γ, are related to each other in the following equations,

$$\frac{ku}{u_*} = ln \frac{z}{z_0} , \tag{19}$$

$$\tau = \rho u_*^2 = \gamma^2 \rho u^2 , \tag{20}$$

$$\Gamma = \left(ln \frac{z}{z_0} \right)^{-1} \text{ (from Eqs. (12) and (18))} \tag{21}$$

Usually, the surface parameter over the water surface is determined by the following three methods:

(a) In neutral conditions, the *vertical profile* of the wind speed (or the water vapour pressure) varies logarithmically with the height near the surface, so that the value of z_0 (or Γ) may directly be determined.

(b) The surface stress is measured by observing the *slope of the water surface* of a lake, pond or wind tunnel. This method, developed by EKMAN (1905), is shown by

$$\sin \psi = \frac{\tau + \tau_b}{g \rho_w d} , \tag{22}$$

where ψ is the slope angle of the water surface, ρ_w the water density, d the mean depth and τ_b the horizontal stress at the bottom.

(c) The method of *geostrophic departure* is used to determine the surface stress of the ocean. This method of estimation from pilot balloon observations, devised by SUTCLIFFE (1936), is shown by

$$\tau_{z=0} = -l \int_0^h \rho (V_g - V) \, dz , \tag{23}$$

where l is the Coriolis parameter, V_g and V the components of the geostrophic and actual wind normal to the direction of the surface wind and h the certain level at which $V_g = V$ is to be satisfied.

This equation is valid when the acceleration is absent.

By each method, many observations have hitherto been made by several workers. Fig. 3 shows the roughness parameter plotted against the interpolated wind speed at 10 m height. The general trend of this figure is reasonable; that is, as the wind speed increases, the roughness parameter increases. This implies that the configuration of the water surface is closely dependent on the wind speed and that with increasing wind speed there occurs an increase in the roughness characteristics of the water surface.

The characteristic of the water wave driven by the wind is a complicated matter. It is a function of the wind speed, duration time of wind, length of wind fetch, wave age and etc. In those factors the wind speed is the main one for the formation of the wave. The relationship between the significant-wave height, H, and the wind speed has been known as an approximate formula, [BRETSCHNEIDER (1952), MUNK and ARTHOR (1951) and etc.],

$$H \fallingdotseq b u^2$$
$$b = 1 \sim 3 \times 10^{-4} \text{ sec}^2/\text{cm} \tag{24}$$

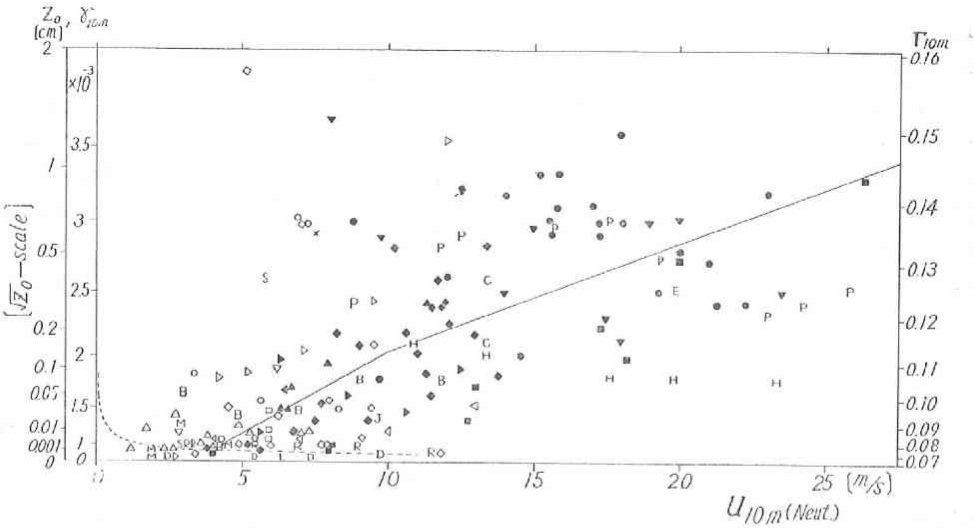

Fig. 3. Variation of the roughness parameter with wind-speed at 10 m level.

Table 2. Symbols used in Fig. 3.

Symbol	Worker		Method
×	Rossby & Montgomery	(1936)	sea: wind profile.
▶	Johnson	(1950)	1 km × 0.5 km, lagoon : wind profile.
■	Francis	(1951)	wind-tunnel.
◇	Sheppard & Omar	(1952)	sea: geostrophic departure.
▼	Hellström	(1953)	28 km × 11 km, Lake Ringköbing Fjord: surface slope.
●	Keulegan	(1953)	390 km × 80 km, Lake Erie (18 m deep): surface slope.
◁	Van Dorn	(1953)	240 m × 60 m, yocht-pond (2 m deep): surface slope.
▷	Brocks	(1955)	ocean: water vapour profile.
◀	Darbyshire et al.	(1955)	10~30 km fetch, Lake Lough Neage: surface slope.
▼	Hay	(1955)	0.8~1.2 km fetch, sea: wind profile.
◆	Deacon et al.	(1956)	sea: wind profile.
□	Fleagle et al.	(1958)	8 km fetch, sea: wind, humidity and temperature profiles.
▽	Ogata and others	(1958)	ocean: wind profile.
△	Takahashi	(1958)	2~30 km fetch, Kagoshima Bay: wind profile.
○	Yamamoto & Kondo	(1960)	10 km, Lake Towada: wind profile.

E, Ekman (1905); S, Shoulejkin (1928);
M, Montgomery (1935); L, Sutcliffe (1936);
P, Palmen (1938): B, Bruch (1940);
H, Hela (1948): D, Durst (1949);
R, Roll (1949); C, Corkan (1950);
J. N.K. Jonson.

} From Francis's Fig. 9 (1951). (field test)

On the other hand, the roughness height for the aerodynamically rough flow measured in pipes uniformly roughened with grains of sand is related with the size of the irregularity, that is $z_0 \fallingdotseq 1/30 \times$(the size of the irregularity). Similarly, the roughness height

measured over the ground surface is found to be an order of magnitude smaller than the actual height of roughness elements, [SUTTON (1953)].

By analogy with the above measurements and from Eq. (24) and Fig. 3 we can deduce that the roughness height of the water surface is related to the wave height, and we can suppose that the size of the significant-wave plays but a small part in the production of aerodynamic roughness, and that the effective height of irregularity is mainly caused by the drag of the bubble-like or small-scale ripples, whose character may primarily be connected with the significant-wave.

From above considerations we will take

$$\left.\begin{aligned} z_0 &= a\, u^2_{10\,n}\ (\text{Neut.}) \\ a &= 1.4 \times 10^{-7}\ \text{sec}^2/\text{cm} \\ \text{for}\quad u_{10\,n}&(\text{Neut.}) = 10\ \text{m/s} \sim 30\ \text{m/s} \end{aligned}\right\} \tag{25}$$

where u(Neut.) represents the wind speed in the neutral condition. In addition, it will be of some interest to compare the two constants, a and b. From Eqs. (24) and (25) we have

$$\frac{a}{b} \fallingdotseq \frac{z_0}{H} \fallingdotseq \frac{1}{1000}$$

For the condition of $u_{10\,n}$(Neut.)$\leq$4m/s we will support an aerodynamically smooth surface, according to observations. In the case of aerodynamically smooth flow, the wind profile obeys the well known VON KARMAN'S formula,

$$\frac{u}{u_*} = \frac{1}{k}\, ln\left(\frac{u_*\, z}{\nu}\right) + 5.5 \tag{26}$$

Eq. (26) may formally be represented as

$$\frac{ku}{u_*} = ln\,\frac{z}{z_0} \tag{27}$$

In this equation z_0 is a formal roughness height for smooth flow. This is shown in Fig. 3 by the dashed curve. For the condition, 4m/s$<u_{10\,n}$(Neut.)$<$10 m/s, we will assume transitional flow. In Fig. 3 the recommended function of z_0 (or $\Gamma_{10\,n}$ or $\gamma^2_{10\,n}$) is shown by the solid line.

Plotted points in Fig. 3 have considerable scatter. This is caused not only by the observational error, but also by the observations which have been done in different conditions of the water surface, (the duration time of wind and etc.), even though during the same wind speed. However, our object is an estimation of the evaporation in the mean condition of the surface such as shown in Fig. 3. As can be seen from the figure, the error induced by the use of z_0 shown in Fig. 3 will be small, because the scatter of plotted points in Γ-scale [$=(lnz/z_0)^{-1}$ scale] is relatively small, and its order of probable errors is considered to be $\pm 10\% \sim 20\%$.

5 Evaporation diagrams

As stated in Section 3 we can make an evaporation diagram by using the turbulent theory and empirical relations. This was done by the following way;

(1) putting u_1(Neut.), [or $u_*=ku_1$(Neut.)$/ln\, z_1/z_0$]

(2) then z_0 may be known as a function of u_1(Neut.),

(3) and assuming a stability parameter ζ_0,

(4) we can know u_1 and $\theta_s-\theta_1$ from Eq. (14) and Table 1, and the value of $E/(\chi_s-\chi_1)$ may be obtained.

Therefore $E/(\chi_s-\chi_1)$ is expressed with u_1 and $\theta_s-\theta_1$. Table 3 shows $E/(\chi_s-\chi_1)$ as functions of u_1 or u_* [or u_1(Neut.)] with parameters of $\theta_s-\theta_1$ or ζ_0. In this Table $z_1=$ 10 m was used. Fig. 4 is the evaporation diagrams. Numbers as parameters are represent $\theta_s-\theta_{10m}$ in °C.

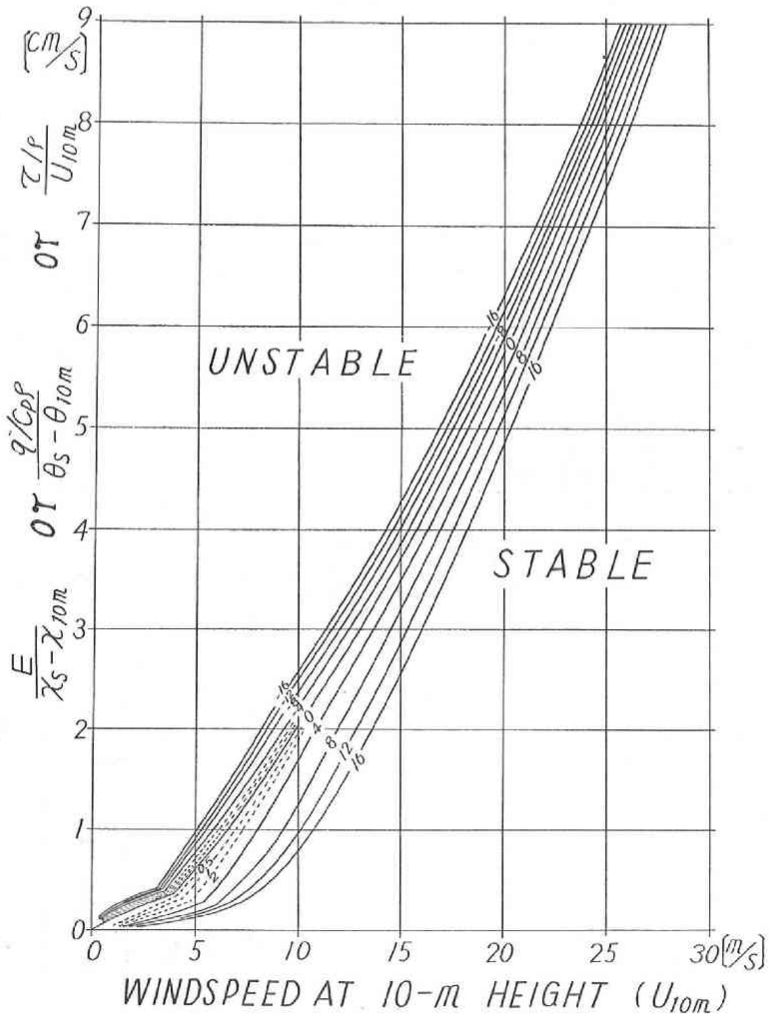

Fig. 4. Evaporation diagrams.

Table. 3 Values of $E/(X_s-X_{10m})$ as a function of u_{10m} (cm/s) with a parameter of $\theta_s-\theta_{10m}$ (°C).

u_*	u_{10m} (Neut)	z_0 \ $\theta_s-\theta_{10m}$		16°C	12°C	8°C	4°C	2°C	1°C	0.5°C	0°C
cm/s	cm/s	cm	u_{10m}	62		66	71	76	81	85	100
3.272	100	.0049	E/X_s-X_{10m}	0.175		0.163	0.151	0.140	0.132	0.125	0.107
			ζ_0	.0067		.0031	.00147	.0007	.00033	.000155	0
6.221	200	.0026	u_{10m}	144		155	164	173	180	187	200
			E/X_s-X_{10m}	0.268		0.248	0.235	0.223	0.215	0.207	0.194
			ζ_0	.00082		.00038	.00017	.000087	.000041	.00002	0
11.85	400	.00137	u_{10m}	330	337	346	360	372	381	388	400
			E/X_s-X_{10m}	0.424	0.416	0.406	0.390	0.378	0.370	0.363	0.354
			ζ_0	.000098	.000073	.000047	.000023	.000011	.0000053	.0000026	0
17.14	500	.0086	u_{10m}	420	429	440	457	471	482	490	500
			E/X_s-X_{10m}	0.701	0.686	0.668	0.642	0.622	0.608	0.598	0.588
			ζ_0	.00034	.00025	.00016	.000079	.000038	.0000185	.0000091	0
27.75	700	.0415	u_{10m}	606	618	633	656	671	683	692	700
			E/X_s-X_{10m}	1.266	1.242	1.212	1.170	1.146	1.126	1.112	1.10
			ζ_0	.00071	.00052	.00034	.00016	.000081	.000041	.00002	0
45.07	1000	.140	u_{10m}	900	915	934	963	980	990		1000
			E/X_s-X_{10m}	2.252	2.217	2.172	2.106	2.070	2.048		2.03
			ζ_0	.00099	.00083	.00048	.00023	.000113	.000055		0
62.26	1300	.236	u_{10m}	1204	1220	1242	1269	1287			1300
			E/X_s-X_{10m}	3.217	3.175	3.118	3.050	3.010			2.983
			ζ_0	.0009	.000665	.000435	.00021	.000104			0
80.65	1600	.358	u_{10m}	1510	1528	1553	1575	1587			1600
			E/X_s-X_{10m}	4.310	4.257	4.195	4.125	4.095			4.06
			ζ_0	.00083	.00062	.00041	.0002	.0001			0
106.8	2000	.56	u_{10m}	1920	1940	1958	1981				2000
			E/X_s-X_{10m}	5.940	5.883	5.825	5.755				5.71
			ζ_0	.00077	.00058	.00038	.00019				0
141.9	2500	.87	u_{10m}	2434	2452	2468	2483				2500
			E/X_s-X_{10m}	8.290	8.230	8.176	8.124				8.07
			ζ_0	.00071	.000535	.00035	.000174				0
179.7	3000	1.26	u_{10m}	2948	2961	2974	2987				3000
			E/X_s-X_{10m}	10.980	10.925	10.878	10.827				10.78
			ζ_0	.00067	.0005	.00033	.000168				0

Table. 3 (Continued)

u_* \ $\theta_s-\theta_{10m}$		−0.5°C	−1°C	−2°C	−3°C	−4°C	−6°C	−8°C	−10°C	−12°C	−14°C	−16°C
cm/s 3.272	u_{10m} $E/\chi_s-\chi_{10m}$ ζ_0	151 0.071 −.000088	170 0.062 −.000154	192 0.055 −.00027		216 0.049 −.00049		242 0.044 −.00088				273 0.040 −.00156
6.221	u_{10m} $E/\chi_s-\chi_{10m}$ ζ_0	244 0.160 −.0000144	266 0.147 −.000028	296 0.131 −.000049	318 0.122 −.000069	335 0.115 −.000088	363 0.106 −.000123	382 0.100 −.000156		410 0.093 −.00022		430 0.089 −.00028
11.85	u_{10m} $E/\chi_s-\chi_{10m}$ ζ_0	418 0.337 −.0000024	445 0.317 −.0000046	485 0.290 −.0000086	515 0.272 −.000012	540 0.260 −.0000153	570 0.246 −.0000215	597 0.235 −.0000275	618 0.227 −.000033	632 0.222 −.0000386	647 0.217 −.000044	658 0.213 −.000049
17.14	u_{10m} $E/\chi_s-\chi_{10m}$ ζ_0	513 0.572 −.0000087	533 0.550 −.0000167	570 0.515 −.0000315	606 0.485 −.000045	631 0.465 −.000057	668 0.440 −.000081	698 0.421 −.000103	730 0.402 −.000123	753 0.390 −.000143	777 0.378 −.000163	796 0.369 −.000181
27.75	u_{10m} $E/\chi_s-\chi_{10m}$ ζ_0	709 1.085 −.000019	721 1.067 −.000037	745 1.035 −.00007	772 0.999 −.000102	797 0.968 −.00013	844 0.911 −.00019	887 0.867 −.00024	921 0.834 −.000293	948 0.810 −.00034	972 0.790 −.00038	994 0.773 −.000425
45.07	u_{10m} $E/\chi_s-\chi_{10m}$ ζ_0		1013 2.002 −.000054	1026 1.977 −.000108	1040 1.947 −.00016	1058 1.916 −.00022	1096 1.849 −.000305	1136 1.785 −.0004	1175 1.726 −.00049	1206 1.680 −.00057	1234 1.642 −.00064	1260 1.609 −.00072
62.26	u_{10m} $E/\chi_s-\chi_{10m}$ ζ_0			1319 2.938 −.000102		1342 2.890 −.0002	1367 2.836 −.00029	1398 2.780 −.00038		1455 2.670 −.00056		1509 2.575 −.00071
80.65	u_{10m} $E/\chi_s-\chi_{10m}$ ζ_0			1614 4.026 −.000098		1632 3.987 −.000194		1672 3.892 −.00038		1717 3.793 −.00056		1763 3.693 −.00072
106.8	u_{10m} $E/\chi_s-\chi_{10m}$ ζ_0					2025 5.628 −.000185		2054 5.550 −.00036		2078 5.480 −.000535		2117 5.395 −.0007
141.9	u_{10m} $E/\chi_s-\chi_{10m}$ ζ_0					2522 8.000 −.000172		2542 7.942 −.00034		2563 7.870 −.00051		2587 7.798 −.00067
179.7	u_{10m} $E/\chi_s-\chi_{10m}$ ζ_0					3017 10.726 −.000168		3035 10.658 −.00033		3052 10.600 −.00049		3068 10.550 −.00065

If we use a certain level different from $z_1=10$ m, or different levels of observations of the wind, the air temperature and the humidity, another diagram will easily be made by the use of Table 3 and the following relations,

$$\frac{u_1}{u_2}=\frac{\chi_s-\chi_1}{\chi_s-\chi_2}=\frac{\theta_s-\theta_1}{\theta_s-\theta_2}=\frac{f_{\xi_1}(\zeta_0)}{f_{\xi_2}(\zeta_0)} \tag{28}$$

Further, from the turbulent theory we get

$$\frac{E}{(1-\varepsilon)(\chi_s-\chi_1)}=\frac{q/c_p\rho}{(1-\varepsilon')(\theta_s-\theta_1)}=\frac{\tau/\rho}{u_1} \tag{29}$$

With the empirical relation, $\varepsilon=\varepsilon'=0$, Eq. (29) may be represented as

$$\frac{E}{\chi_s-\chi_1}=\frac{q/c_p\rho}{\theta_s-\theta_1}=\frac{\tau/\rho}{u_1} \tag{30}$$

Thus the turbulent flux of heat or the surface stress may be calculated by the same diagrams.

References

Bretschneider, C.L., 1952: The generation and decay of wind waves in deep water. Trans. Amer. Geophys. Uni., **33**, 381.

Brocks, K., 1955: Wasserdampfschichtung über dem Meer und "Rauhigkeit" der Meeresoberfläche. Arch. Meteorol. Geophys. Biok., (A), **8**, 354.

Darbyshire, J. and Mollie Darbyshire, 1955: Determination of wind stress on the surface of Lough Neagh by measurement of tilt. Quart. J.R. Met. Soc., **81**, 333.

Deacon, E.L., P.A. Sheppard, E.K. Webb, 1956: Wind profiles over the sea and the drag at the sea surface. Australian J. Phys., **9**, 511.

Ekman, V.W., 1905: On the influence of the earth's rotation on ocean-currents. Ark. Mat. Astr. Fys., 2, No. 11, 1.

Fleagle, R.G., J.W. Deardorff and F.I. Badgley, 1958: Vertical distribution of wind speed, temperature and humidity above a water surface. J. Marine Res., **17**,141.

Francis, J.R.D., 1951: The aerodynamic drag of a free water surface. Proc. Roy. Soc. A, **206**, 387.

Hay J.S., 1955: Some observations of air flow over the sea. Quart. J. R. Met. Soc., **81**, 349.

Hellström, B., 1953: Wind effect on Ringköbing Fjord. Trans. Amer. Geo. Uni., **34**, 194.

Johnson, J.W., 1950: Relationships between wind and waves, Abbottes Lagoon, California. Trans. Amer. Geo. Uni., **31**, 386.

Kao, Shih-Kung, 1959: Turbulent transfer in the boundary layer of a stratified fluid. J. Met. **16**, 497.

Keulegan, G.H., 1953: J. Res. Bur. Stand., Washington, **50**, 95.

Kondo, J., 1962: Observations on wind and temperature profiles near the ground. Sci. Repts. Tohoku Univ., Ser. 5, Geophys. **14**, 41.

Montgomery, R.B., 1940: Observations of vertical humidity distribution above the ocean surface and their relation to evaporation. Pap. Phys. Ocea. Met. Mass. Inst. Technol. and Woods Hole Oceanog. Inst., **7**, 4.

Munk, W.H. and R.S. Arthur, 1951: Forcasting ocean waves. Compendium of Meteorology, 1982, Ame. Met. Soc.

Ogata, T. and Others, 1959: On the meteorological condition near the sea surface at "Tango". J. Met. Res. **11**, 607, (in Japanese).

Rossby, C.G., and R.B. Montgomery, 1936: On the momentum transfer at the sea surface.

Papers in Phys. Oceanogr. and Met. Cambridge, Mass., **4**, 1.

SHEPPARD, P.A. and M.H. OMAR, 1952: The wind stress over the ocean from observations in the Trades. Quart. J. R. Met. Soc., **78**, 583.

SUTCLIFFE, R.C., 1936: Surface resistance in atmospheric flow. Quart. J.R. Met. Soc., **62**, 3.

SUTTON, O.G., 1953: Micrometeorology. New York: McGrow-Hill Book Co.

SYÔNO, S. and M. HAMURO, 1962: Notes on the wind-profile in the lower layer of a diabatic atmosphere. J. Met. Soc. Japan, II, **40**. 1.

TAKAHASHI, T., 1958: Micro-meteorological observations and studies over the sea. Memoirs of the Faculty of Fisheries, Kagoshima Univ. **6**, 1.

THORNTHWAIT, C.W. and B. HOLZMAN, 1939: The determination of evaporation from land and water surfaces. Monthly Weather Rev., **67**, 4.

VAN DORN, W., 1953: Wind tides on an artificial pond. J. Marine Res., **12**, 249.

YAMAMOTO, G., 1959: Theory of turbulent transfer in non-neutral conditions. J. Met. Soc. Japan., II, **37**, 60.

YAMAMOTO, G. and J. KONDO, 1960: Evaporation from Lake Towada, Secondary report: Sendai: Tohoku Electric Power Co., (in Japanese).